



## Sparse Non-stationary Thermal Wave Imaging for GFRP

Md M Pasha<sup>1,2</sup>, G V S Rao<sup>1</sup>

<sup>1</sup>Infrared Imaging Center, Department of Electronics and Communication Engineering, Koneru Lakshmaiah Education Foundation, Vaddeswaram, AP, India, [urspasha@gmail.com](mailto:urspasha@gmail.com)

<sup>2</sup>KSRM College of Engineering, Andhra Pradesh, India.

### ABSTRACT

Active thermography is evolving as an efficient testing method for inspection of various materials with rapid development of infrared imaging technologies. Traditionally thermal response is captured at a rate determined by the IR camera which leads to data redundancy and consumption of resources. In this paper thermal response of a Glass Fibre Reinforced Polymer (GFRP) at a reduced rate is captured by applying Compressive Sensing (CS) to Quadrature Frequency Modulated Thermal Wave Imaging (QFMTWI). Convex optimization algorithm Basis Pursuit (BP) solves L1 norm minimization to recover the complete thermal response. Recovered thermal response is processed using pulse compression approach to inspect the defects in the GFRP test sample. To quantify the effectiveness of defect detectability of this method SNRs of the defects for original and recovered thermal response are compared.

**Key words:** Active Thermography, Basis Pursuit, Compressive sensing, Frequency Modulated Thermal Wave Imaging.

### 1. INTRODUCTION

Now a days fibre reinforced composite materials finds its applications in automotive, avionics and civil infrastructure. Due to low weight, high stiffness and high protection against corrosion, they are used in applications involving retrofitting of structures and avionics. But due to presence of inescapable defects such as voids and delaminations formed during manufacturing curbs their use in applications and requires detailed inspection prior to deployment. From the available non-destructive evaluation procedures for testing of these materials infrared thermography [1] - [12] is becoming popular due to its reliable testing procedure. In this method of testing surface temperatures are mapped as heat flows through the test sample, to detect surface and subsurface defects. This method is fast non-contact method of defect identification. Infrared thermography is broadly classified in to active and passive methods [1]. In passive approach natural temperature difference between ambient and sample to be certified is obtained. This method cannot detect flaws lying deep interiors of the material. To overcome this, active

thermography on the other hand uses external energy stimulation on the material to be tested. Pulsed thermography (PT) [3] – [5], modulated lock-in thermography(LT) [2], pulsed phase thermography(PPT) [4] and frequency modulated thermal wave imaging(FMTWI) [15] [16] are some of the approaches in active thermography. PT works with high peak power heat sources and is prone to surface radiation alterations and has non uniform warming on the surface of material being inspected. In LT a mono frequency thermal wave excitation based on the thermal characteristic and geometry of sample, launches extremely attenuated dispersive signals of the identical frequency into the sample. Reflected thermal wave image sequence is recorded and phase information is derived. LT has the inherent drawback that to distinguish defects at various depths experiment needs to be conducted multiple number of times with different frequency excitations. PPT is same as PT, but the different frequency components are extracted by performing Fourier transform at each of the pixel location of the thermal image sequence. With an objective to detect defects present deeper in test samples, PT and PPT depend upon high pulsed power heat sources which damages materials under test [13] [14]. In FMTWI approach desired range of frequencies (linear chirp) are launched in to the sample in a single go. FMTWI is similar to radar pulse compression [17] approach using which good depth resolution can be obtained. The key principle in this approach is that if the two defects lies at different depths, then the arrival of reflected signals differ in time. This time delay or group delay is obtained by cross correlating the thermal profile of non-defective location of the test sample with all other profiles. However the presence of large sidebands in linear FMTWI causes decrease in SNR of the defects which is overcome by Quadrature Frequency Modulated Thermal Wave Imaging (QFMTWI) [18]. Pulse compression has convenience of long range detection and superior range resolution as obtained with long pulse and short pulse respectively. In pulse compression approach the reflected signal from the target is passed through a matched filter whose impulse response is replica of the response of reflected signal. The output of matched filter will be a narrow peak termed compressed pulse. The resolution capability of matched filter increases with decrease in bandwidth and vice-versa.

Correlation method can also be used to compute the pulse compression. In this method time delay is obtained by cross correlating the reference signal with the delayed

received signal. If the reference signal is symmetric both methods gives the same result [19]. Generally finding peak of the correlation function is to be done on the sampled data, this indicates that cross correlation function must be sampled on a discrete grid. To obtain this the reflected sampled signal is multiplied on to a dictionary of reference signals, each one of which is a delayed version of known reference signal. Time delay can be estimated by searching the correlation vector for maximum non- zero components. To attain good depth resolution high sampling rate is required which may be costly. In many applications including thermography the dimension of the sampled signal may be much greater than the information conveyed by it. Therefore signal may be assumed sparse and there is a possibility to reduce the sampling rate by using compressive sensing (CS) [20]-[23]. CS has the potential to collect the necessary information for faithful recovery of compressible or sparse signal using low dimensional non-linear projections.

In this paper CS based thermal wave detection is applied for inspection of defects in Glass Fiber Reinforced Polymer (GFRP) test sample. Thermal response is captured using low frame rate IR camera and later using convex optimization based Basis Pursuit (BP) [24] [25] recovery algorithm entire thermal response is reconstruct. Reconstructed thermal response is processed using Pulse Compression technique for inspection of defects and SNRs of the defects are compared among Original and reconstructed thermal data to test the effectiveness of the CS based recovery.

## 2. COMPRESSIVE SENSING

CS recovers signals and parameters from an under-determined system of linear equations using sparsity as a constraint in a known basis. Let  $X$  is a  $N$  dimensional signal with a maximum of  $K$  non-zero components. This signal is said to be  $K$  sparse. To obtain information of a signal  $X \in \mathbb{C}^n$ ,  $M < N$  measurements  $\phi_m, m = 1, 2, \dots, M$  are applied to  $X$  so that  $y_m = \phi_m^T X$ . Suppose sensing waveforms are obtained in a  $M \times N$  sensing matrix  $\theta = (\phi_1 \phi_2 \dots \phi_M)$ , then the sampling process is expressed by the equation  $Y = \theta X$ . Let the basis function  $\psi_n, n = 1, 2, \dots, N$  be introduced for the signal:  $X = \sum_{i=1}^N a_i \psi_i$ , and in matrix form  $X = \Psi a$  where  $a$  is coefficient vector and  $N \times N$  matrix  $\Psi = (\psi_1 \psi_2 \dots \psi_N)$ . The measurement can be expressed with respect to coefficients  $Y = \theta X$  where  $\theta = \theta \Psi$ . Since the measurements  $M$  are much smaller than the length  $N$  of the signal  $X$ , this situation is underdetermined.

### 2.1 Basis Pursuit

The sparse recovery problem can be viewed as recovering of  $K$ -sparse signal  $X$  from the measurements  $Y=AX$ . Easiest way to recover this vector is to solve the  $l_0$  minimization problem.

$$\min \|X\|_0 \text{ subject to } AX=Y \quad (1)$$

This  $l_0$  minimization problem works good in theory. However it is not numerically solvable and is NP- Hard in

general. If  $l_0$  minimization is replaced with the  $l_1$  minimization i.e.

$$\min \|X\|_1 \text{ subject to } AX=Y \quad (2)$$

Candes and Tao illustrated in [27] that when measurement matrices satisfy Restricted Isometry Property (RIP),  $l_1$ -norm minimization recovers all sparse signals exactly, this is basis pursuit algorithm. In general exact sparse signals are not encountered and also measurements and signals are noisy. Candes and his associates showed in [28] that a variant of Basis Pursuit called Basis Pursuit De-Noiseing (BPDN) which approximately recovers signals affected by noise.

$$\min \|X\|_1 \text{ Subject to } \|AX - Y\|_2 \leq \epsilon \quad (3)$$

Where  $\epsilon$  is proportional to variance of noise.

Matrix  $A$  satisfies RIP of order  $M$  if there exist a  $\delta_M \in (0,1)$  such that

$$(1-\delta_M) \|x\|_2^2 \leq \|Ax\|_2^2 \leq (1 + \delta_M) \|x\|_2^2 \quad (4)$$

holds for all  $x \in \sum_M$

RIP of matrix  $A$  can be verified using coherence property, which is defined as

$$\mu = \max_{i \neq j} | \langle a_i, a_j \rangle | \quad (5)$$

where  $a_i$  and  $a_j$  are any two columns of  $A$ .

There are various algorithms to solve the convex optimization problem involving  $l_1$ . In [25] authors show that among various algorithms simplex and Interior Point methods give good results for this optimization problem.

The simplex method is variation of Dantzig's algorithm. Initially a new Matrix  $\hat{A}$  is constituted such that its columns are linearly independent to columns of  $A$ . Therefore the corresponding solution  $\hat{A}^{-1}y$  is feasible. Then iteratively basis  $\hat{A}$  is improved by swapping one column in basis by one column not in basis such that swap improves the desired property of solution. There are many ways such as anti-cycling rules by which one can select column to swap in such a manner that convergence to optimal solution is guaranteed.

The interior point method starts from a solution to  $Ax_0 = y$  where  $x_0 > 0$ . Then entries in  $x_{k-1}$  are changed through an iteration process to obtain the solution  $x_k$  such that the condition  $Ax_k = y$  is satisfied.  $x_k$  is projected on to a basis matrix such that resulting signal is sparse. By limiting smaller values to zero at a particular iteration a vector is obtained which satisfies the stopping criteria which forms the solution.

Random matrices  $A$  whose entries are independent and identically distributed (i.i.d) Gaussian entries with zero mean and variance  $1/N$  satisfies RIP and can guarantee the exact recovery of  $x$  with overwhelming probability. Gaussian, Bernoulli or sub gaussian random projections are such matrices. For Gaussian and Bernoulli matrices, RIP holds for  $K \approx M/\log(N/M)$ . For structured matrices, such as random section of a discrete fourier transform, RIP holds when  $K \approx M/\log^p(N)$ .

There are many solvers available to solve this problem involving  $l_1$ . The matlab software packages  $l_1$  magic [29],

CVX [30], Sparse lab[ 31], YALL1 [32] and LASSO [33] are some of the solvers. In our work CVX matlab package is used.

### 3. PROBLEM FORMULATION

This paper studies the application of CS to the thermographic data. Thermal response from the test sample is captured at reduced frame rate and complete data is recovered using compressive sensing based Basis Pursuit algorithm. Recovered thermal data is processed using pulse compression based method for defect detection and performance is analysed.

#### 3.1 Compressive Sensing Applied to Thermography

Compressive sensing theory is described in previous section. In our work IR camera acquires thermal response of the test sample at a constant frame rate and thereby a video signal with total number of frames depending on the time the test sample is exposed to radiation is captured. Fig. shows the video signal illustration as captured by the IR camera. Suppose there are  $N$  frames in this video signal. Now compressed thermal response at a reduced frame rate is obtained by projecting the video on to a measurement matrix. Thermal response at a pixel location  $x$  is projected on to a random measurement matrix to obtain a compressive signal  $y$ . The set of locations which are retained in this step are used to obtain the complete compressed thermal response at a reduced rate. To obtain compressed measurements directly arrangement must be made in the camera sensors to capture the compressed response. From this compressed response complete data must be recovered using  $l_1$  minimization as described in Eq. 2. The thermal response at pixel location is represented by  $X$  in Eq. 2 and it is a column vector. The  $M \times N$  measurement matrix  $\Phi$  is obtained by sampling i.i.d entries of a normal distribution with mean zero and variance  $1/M$  as described in the previous section. Sparsity level  $K$  is determined experimentally from the thermal data and the sparsifying dictionary  $\Psi$  in our work is DFT matrix. Given the measured signal  $y$  from the availability of the measurement matrix  $\Phi$  and the sparsifying dictionary  $\Psi$   $l_1$  norm is minimized using basis pursuit algorithm and  $N$  dimensional coefficient vector  $a$  is recovered and from this complete signal  $x$  is recovered. To select the optimum value of  $M$  reconstruction is done with various measurements such as  $2*K$ ,  $3*K$ , etc. so on at a chosen pixel location. The value of  $M$  which gives least mean square error is selected for capturing entire thermal response.

#### 3.2 Compressive Sensing Recovery Algorithm

Basis Pursuit is described in section II. Compressive sensing recovery using basis Pursuit is summarized here.

- Compressive measurements  $y$  from the captured thermal response is obtained as described in the previous section.

- At each pixel location coefficient vector  $a$  is recovered by solving  $l_1$  norm minimization using Basis Pursuit.
- Inverse DFT is applied on the coefficient vector  $a$  to obtain the thermal profile  $x$ .

Above steps are repeated for all the pixel location of the thermal response to recover the complete video signal.

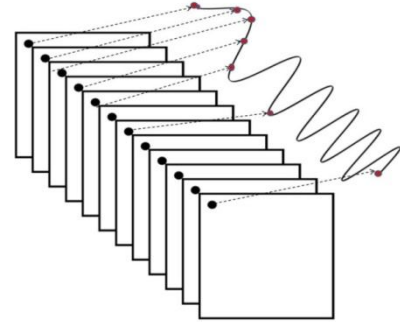


Figure 1: Illustration of video signal captured by IR camera

#### 3.3 Pulse Compression for Thermal Wave Imaging

Pulse compression is most popular method in radio detection and ranging (RADAR) engineering to obtain good range resolution, sensitivity and signal to noise ratio. Using this detection range and resolution is obtained with long duration low peak power pulse as achieved with short duration high peak power pulse in the influence of noise. Let  $r(t)$  be a signal which is being reflected from a subsurface defect in the test object after being exposed with a LFM excitation. This signal is same as the signal reflected at a non-defective location except for some attenuation in magnitude and with a fixed delay. Let this signal be represented as a reference signal  $h(t)$ . When signal  $r(t)$  is cross-correlated with  $h(t)$  it produces an output  $g(t)$  which is a narrow peak called compressed pulse whose peak is located at a delayed location based on the delay between  $r(t)$  and  $h(t)$ .

The cross correlation of the reference signal (impulse response) and the received signal, is given by:

$$g(\tau) = \int_{-\infty}^{\infty} r(t)h(\tau + t)d\tau \quad (6)$$

For two defects lying at distinct depths their corresponding reflected signals differ in both amplitude and time. Due to this compressed pulse peaks corresponding to these defects are observed at different time instants, and measure of defect depth is proportional to occurrence of compressed pulse peak. In correlation approach developed temperature distribution over a reference region as a result of heat excitation can be treated analogous to  $r(t)$  and the consequence temperature distribution developed at the region of defect is identical to  $h(\tau+t)$ . Therefore time delay can be obtained by response of cross-correlation given by Equation 15.

To apply pulse compression using this method, at each pixel location average rise in temperature by cause of active heating is estimated and compensated by fitting the data to the thermal profiles. Then cross-correlation is applied between the each of the mean removed pixel and reference thermal profile. As a result normalized correlation coefficients are obtained and are preserved at the corresponding locations. These deviations in the correlation coefficients help to detect subsurface defects.

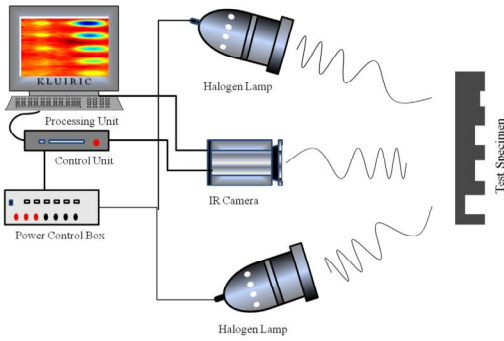


Figure 2: Experimental Setup

#### 4. EXPERIMENT

Experimentation is conducted on a Glass Fibre Reinforced Polymer (GFRP) test sample to obtain the data which is processed for defect detection. A control unit connected to a set of halogen lamps of power 1 kW each generates QFM thermal excitation in the range 0.01 to 0.1 Hz which is focussed on to the test sample. Temporal thermal response of the test sample is captured using an infrared camera FLIR SC 655 A with spectral range 5 to 8 μm and at a frame rate of 25 frames per second over a period of 100 s. The experimentation setup is shown in the Fig. 2. The test sample used in our experimentation is a GFRP specimen consisting of embedded patches, water ingress and cracks.

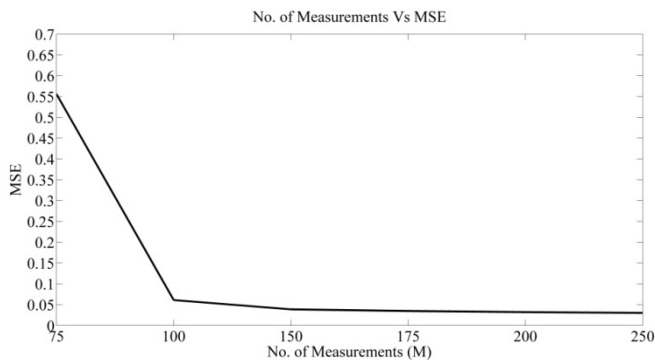


Figure 3: MSE plot

#### 5. RESULTS AND DISCUSSION

Reconstruction procedure based on basis pursuit is explained in section. The IR camera captures thermal response from the test sample at a period of 25 frames per second with a spatial resolution of 104 x 98 for 100 s so that 2500 frames are generated. The basis matrix  $\Psi$  used for sparsifying the signal is DFT. The random measurement matrix of dimension  $M \times$

2500 for various values of  $M$  based on sparsity level  $K$  is generated. The sparsity level is calculated experimentally from the given data and for our thermographic data it is found to be 25. At a chosen pixel location of the thermal response various measurements  $M$  with multiple values of sparsity level  $K$  are generated. For each value of  $M$  Basis Pursuit reconstruction algorithm is applied and mean square error (MSE) is computed. Fig. 3. shows MSEs of the reconstructed signal for various measurements. It can be observed from the MSE plot that with  $10 \times K$  i.e. 250 measurements MSE is minimum. Using this value of  $M$  compressive measurements for the entire thermal response is obtained and by applying Basis Pursuit reconstruction algorithm as described in section IV complete thermal response is reconstructed. Fig. 4. shows compressed and reconstructed thermal profile with  $M=250$  measurements with QFM excitation signal. In reconstructed thermal profiles retaining spectral components is crucial as most of the information about the defects is preserved in it. As the excitation frequency is from 0.01 Hz to 0.1 Hz preserving frequency components in this range is required which is achieved as can be seen from the frequency spectrum plot of Fig. 5. Reconstructed thermal data using basis pursuit is then processed with correlation based pulse compression for inspection of defects in GFRP test sample. Frame highlighting the defects is then chosen subjectively from the series of thermograms. Fig. 6. shows frames highlighting defects in the GFRP test sample after processing original, compressed and reconstructed thermal data using pulse compression method. In this figure a, b and c are the manually embedded patches in to the test sample, d and e shows water ingress formed into the sample and f and g are the cracks. SNRs of the manually embedded defects are computed to quantify the visibility of the defects at each of the locations of defects using

$$SNR(dB) = 20 \log \left( \frac{\text{Mean of the defect area} - \text{mean of the non defective area}}{\text{Standard deviation of non defective region}} \right)$$

Fig. 7. shows the SNR comparison of embedded defects in the test sample for original and reconstructed thermal data using basis pursuit. It can be noticed from the SNR comparison that SNRs of the defects in the reconstructed thermal data are very close to original. With measurements as few as one-tenth of the original data satisfactory reconstruction using basis pursuit algorithm and inspection of defects using pulse compression is possible.

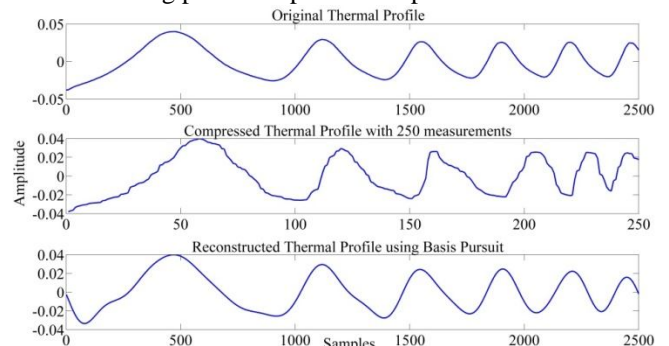
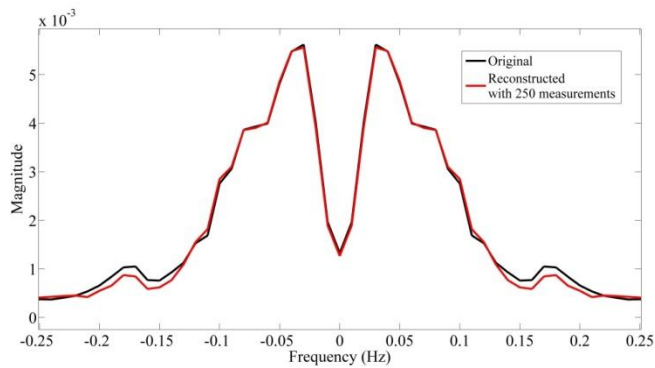
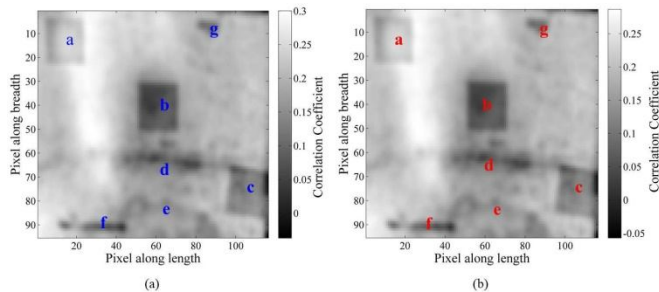


Figure 4: Compressed and Reconstructed Thermal Profile using 250 measurements



**Figure 5:** Frequency Spectrum of original and reconstructed thermal profile at a pixel location



**Figure 6:** Pulse compressed image at group delayed instant of 9 sec (a) Original Data (b) Reconstructed data using Basis Pursuit with 250 measurements

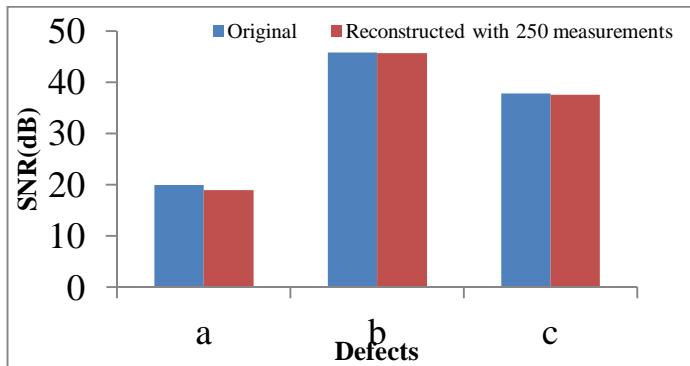


**Figure 7:** SNR comparison of the defects from Original and Reconstructed data using Pulse Compression

## 6. CONCLUSION

This paper puts light on application of CS based Basis Pursuit recovery algorithm to reconstruct thermal response at a reduced frame rate. Thermal response at a reduced rate is obtained from the original thermal response and then using Basis Pursuit recovery algorithm complete thermal response is reconstructed and further using pulse compression approach defects were identified successfully. Original thermal response has 2500 frames and after compressed sensing they were reduced to 250 frames, thus it leads to memory saving as well as saving of sensor resources and power. Even though convex optimization based Basis Pursuit is computationally complex, non convex methods like greedy and iterative algorithms can be used for fast computing. It can be concluded that if efficiently used CS has lot of

potential in thermography applications which can save resources such as power and memory.

## REFERENCES

1. X P V Maldague. *Theory and Practice of Infrared Thermography for Non destructive Testing*. Wiley-Interscience, Hoboken, 2001
2. G. Busse and P. Eyerer. **Thermal wave remote and nondestructive inspection of polymers**. *Appl.Phys. Lett.*, vol. 43, no. 4, pp. 355–357, 1983. <https://doi.org/10.1063/1.94335>
3. N. P. Avdelidis and D. P. Almond. **Through skin sensing assessment of aircraft structures using pulsed thermography**. *J. NDT & E Int.*, vol. 37, no. 5, pp. 353–359, 2004. <https://doi.org/10.1016/j.ndteint.2003.10.009>
4. C. Ibarra-Castanedo, N. P. Avdelidis, and X. Maldague. **Qualitative and quantitative assessment of steel plates using pulsed phase thermography**. *J. Mater. Eval.*, vol. 63, no. 11, pp. 1128–1133, 2005.
5. R. Mulaveesala, S. Awasthi, and S. Tuli. **Infrared non-destructive characterization of boiler Tube**. *Sensor Lett.*, vol. 6, pp. 1–6, 2006.
6. N. P. Avdelidis and D P Almond. **Through skin sensing assessment of aircraft structures using pulsed thermography**. *J NDT&E International*, 37(5), pp 353-359, 2004. <https://doi.org/10.1016/j.ndteint.2003.10.009>
7. S. M. Shepard. **Advances in pulsed thermography**. *SPIE*, Vol 4360, pp 511-515, 2001. <https://doi.org/10.1117/12.421032>
8. A Rosencwaig and A Gersho. **Theory of the photoacoustic effect in solids**. *J Appl Phys*, Vol 47, p 64, 1976. <https://doi.org/10.1063/1.322296>
9. S. D. Cowell, D D Burleigh and T J Murray. **Flash lamp heat flux requirements for thermographic inspection of fibre composite laminates**. In *Proceedings of SPIE*, 1094, pp 182-187, 1989. <https://doi.org/10.1117/12.953401>
10. D. P. Almond and S. K. Lau. **Defect sizing by transient thermography. I: an analytical treatment**. *Journal of Physics D: Applied Physics* 27, pp 1063-1069, 1994.
11. M. B. Saintey and D. P. Almond. **Defect sizing by transient thermography. II: a numerical Treatment**. *Journal of Physics D: Applied Physics* 28, pp 2539-2546, 1995. <https://doi.org/10.1088/0022-3727/28/12/023>
12. N. P. Avdelidis, B. C. Hawtin and D. P. Almond. **Transient thermography in the assessment of defects of aircrafts composites**. *NDT&E International*, 36 (6), pp 433-439, 2003.
13. H. I. Ringermacher, D. R. Howard and R. J. Filkins. **Flash-quenching for high-resolution thermal depth imaging**. In *AIP Proceedings*, Vol 700, Issue 1, pp 477-481, 2004. <https://doi.org/10.1063/1.1711660>

14. H. I. Ringermacher, D. R. Howard and B. Knight. **Thermal imaging at General Electric.** In *AIP Proceedings*, Vol 820, Issue 1, pp 523-528, 2006.
15. R. Mulaveesala and S. Tuli. **Theory of frequency modulated thermal wave imaging for non-destructive sub-surface defect detection.** *Appl. Phys. Lett.*, vol. 89, no. 19, pp. 1913–1913, 2006.
16. V. S. Ghali and R. Mulaveesala. **Frequency modulated thermal wave imaging techniques for non-destructive testing.** *Insight* Vol 52 No 9, pp. 475-480 September 2010. <https://doi.org/10.1784/insi.2010.52.9.475>
17. M. Skolnik. **Radar Handbook.** New York, NY, USA: McGraw Hill, 1970.
18. Ghali V. S. and Mulaveesala R. **Quadratic frequency modulated thermal wave imaging for non-destructive testing.** *Prog. Electromagn.Res.*, vol. 26, pp. 11–22, 2012.
19. R. Mulaveesala, J. S. Vaddi and P. Singh. **Pulse compression approach to infrared non-destructive characterisation**, *Rev Sci Instrum*, Vol 79, No 9, p 4901, 2008.
20. E. Candès, J. Romberg, and T. Tao. **Robust uncertainty principles: Exact signal reconstruction from highly incomplete frequency information.** *IEEE Trans. on Information Theory*, vol. 52, no. 2, pp. 489–509, 2006.
21. D. Donoho. **Compressed sensing.** *IEEE Trans. on Information Theory*, vol. 52, no. 4, pp.5406–5425, 2006.
- 22 E.J. Candès, and J. Romberg. **Sparsity and incoherence in compressive sampling**, *Inverse Problems*, 23 (3) (2007) 969–985.
23. E. Candès, and M. Wakin. **An introduction to compressive sampling [a sensing/sampling paradigm that goes against the common knowledge in data acquisition].** *IEEE Signal Processing Magazine* 25 (2) (2008) 21–30. <https://doi.org/10.1109/MSP.2007.914731>
24. Stephen Boyd, and Lieven Vandenberg, **Convex Optimization**, Cambridge University Press, 2004, ISBN 9780521833783, pp. 337-3 37
25. S. S. Chen, D. L. Donoho, and M. A. Saunders. **Atomic decomposition by basis pursuit.** *SIAM J. Sci. Comput.*, 20:33–61, 1999.
26. H. Carslaw and J. Jaeger. **Conduction of heat in solids:** Oxford Science Publications. Oxford, England, 1959.
27. E. Candès and T. Tao. **Decoding by linear programming.** *IEEE Trans.Inform. Theory*, vol. 51, no. 12, pp. 4203-4215, Dec. 2005. <https://doi.org/10.1109/TIT.2005.858979>
28. E. Candès, J. Romberg, and T. Tao. **Stable signal recovery from incomplete and inaccurate measurements.** *Communications on Pure and Applied Mathematics*, 59(8):1207–1223, 2006.
29. Candès Emmanuel. **11-magic : Recovery of sparse signals via convex programming.** *Caltech* (2005).
30. [www.cvxr.com](http://www.cvxr.com) [online]
31. [www.sparselab.stanford.edu](http://www.sparselab.stanford.edu) [online]
32. Wei Deng, Wotao Yin, and Yin Zhang. **Group Sparse Optimization by Alternating Direction Method.** *TR11-06, Department of Computational and Applied Mathematics, Rice University*, 2011) <https://doi.org/10.21236/ADA585746>
33. Tibshirani, R. **Regression shrinkage and selection via the lasso.** *J. Royal. Statist. Soc B.*, Vol. 58, No. 1, pages 267-288).
34. R. Jaya Lakshmi et al.. **Bartlett Windowed Quadratic Frequency Modulated Thermal Wave Imaging.** *IJETER*, Vol. 7, No. 11, November 2019, pages 512 – 516. <https://doi.org/10.30534/ijeter/2019/187112019>
35. Eko Julianto, Waluyo Adi Siswant, Marwan Effendy. **Characteristics of Temperature changes and Stress of Float Glass under Heat Radiation**, *International Journal of Emerging Trends in Engineering Research*, Volume 7, No. 9 September 2019. <https://doi.org/10.30534/ijeter/2019/03792019>
36. Hazel Mae A. Adriano, Dustin A. Reyes, Kristelee Jem B. Tan, Daniel D. Zagada, Reggie C. Gustilo. **Defensive Turret Defensive Turret with Fully Automated Motion Detection Using Infrared Technology.** *International Journal of Emerging Trends in Engineering Research*, Volume 7, No. 9 September 2019. <https://doi.org/10.30534/ijeter/2019/05792019>